Journal of the European Ceramic Society 42 (2022) 5624–5630

Contents lists available at ScienceDirect

Journal of the European Ceramic Society

journal homepage: www.elsevier.com/locate/jeurceramsoc

Microwave sintering study of strontium-doped lanthanum manganite in a single-mode microwave with electric and magnetic field at 2.45 GHz

Sheila Moratal [a], Rut Benavente [a], María D. Salvador [a], Felipe L. Peñaranda-Foix [b], Rodrigo Moreno [c], Amparo Borrell [a,*]

[a] Instituto de Tecnología de Materiales (ITM), Universitat Politècnica de València, Camino de Vera, s/n, 46022 Valencia, Spain
[b] Instituto de las Tecnologías de la Información y Comunicaciones (ITACA), Universitat Politècnica de València, Camino de Vera s/n, 46022 Valencia, Spain
[c] Instituto de Cerámica y Vidrio, CSIC, Kelsen 5, 28049 Madrid, Spain

ARTICLE INFO

Keywords:
Microwave sintering
LSM
Mechanical properties
Magnetic heating

ABSTRACT

The objective of this work is to study the changes in the physical and mechanical properties of strontium-doped lanthanum manganite (LSM) material and LSM-YSZ (ZrO_2 doped with 8 mol% yttria) composite, obtained by colloidal processing and sintered by 2.45 GHz microwave sintering at 1200 and 1300 °C using two different single-mode cavities. One circular cavity with TE_{111} mode that has maximum in the electric field (*E*-field) and one rectangular cavity with TE_{102} mode that has maximum in the magnetic field (*H*-field). As compared to conventional sintering at 1300 and 1400 °C, the microwave-heated samples exhibited a denser structure for shorter sintering times. LSM-based materials showed higher heating behavior in *H*-field, which translates into higher energy absorption. This fact can be attributed to an electromagnetic pressure induced by the combined effect of current loops subjected to *H*-field. Therefore, the interaction between the material and the electromagnetic waves depends on the dominant field of them.

1. Introduction

Strontium doped lanthanum manganite (LSM) with general formula $La_{1-x}Sr_xMnO_3$ belongs to the family of perovskite materials. Manganite-based perovskite-type oxides have attracted much attention for the different technological applications that can be built through their peculiar electronic and magnetic features [1,2]. Technically applied stoichiometries have been developed based on a compromise between their conductivity, thermo-chemical properties and long-term chemical stability, as well as their electrochemical properties within composites [3,4]. LSM exhibits ferromagnetic behaviour at room temperature due to properties like the colossal magnetoresistance and magnetocaloric effect [5]. Unfortunately, LSM materials exhibit poor ionic conductivity [6].

Some material properties such as ferromagnetism and electronic conductivity are fundamental for the sinterability by microwave technology. Electromagnetic waves are composed by an electric field (*E*) and a magnetic field (*H*) that are perpendicular to each other. The processing of a material using microwave technology depends on its dielectric and magnetic properties as the electric field and magnetic field components interact with the material during irradiation [7]. The mechanism of heat generation during microwave-material interaction is complex. The electric and magnetic field components of microwave induce changes in the orientation, position and motion of dipoles, free electrons, domain wall and electron spin during material processing [8]. The electric field component of microwave is responsible for the dielectric heating. In the frequency range of microwaves, the dielectric heating is affected via two primary mechanisms, dipolar polarization and ionic conduction. The dipolar polarization mechanism is the primary principle of microwave dielectric heating that involves the heating of electrically insulating materials by dielectric loss [9]. In the conduction mechanism, an electric current is created due to the movement back and forth of the mobile charge carriers under the effect of the microwave *E*-field.

Recently, the microwave magnetic field (*H*) heating has received increasing attention over the electric field heating due to its superior advantages for some materials [10]. Peng et al. reported that microwave magnetic field was more efficient than electric field and magnetic loss can be in the order of four times greater than the dielectric loss in the microwave heating of ferrites [10]. Furthermore, in microwave heating of ferromagnetic powders a strong contribution by the *H*-field interaction with matter has been reported, which can be significantly higher

* Corresponding author.
E-mail address: aborrell@upv.es (A. Borrell).

https://doi.org/10.1016/j.jeurceramsoc.2022.05.060
Received 30 March 2022; Received in revised form 23 May 2022; Accepted 24 May 2022
Available online 25 May 2022

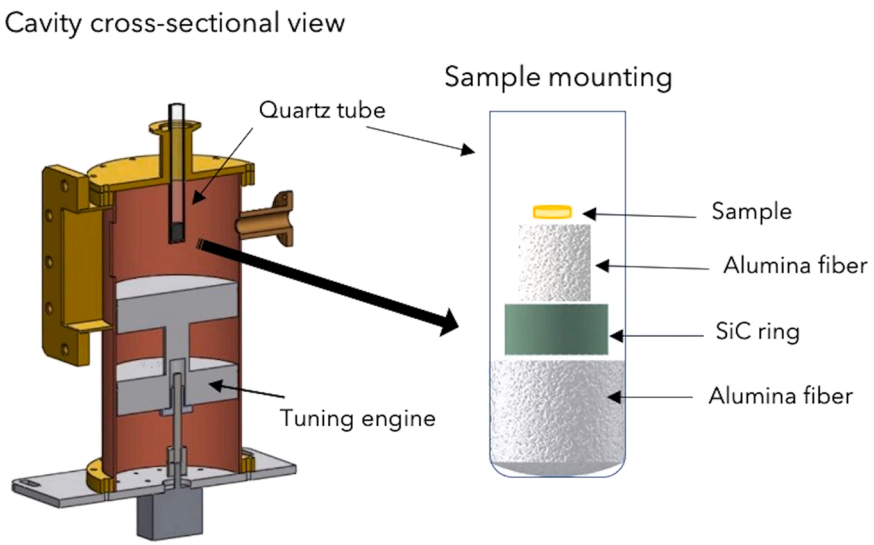

Fig. 1. Detail of the sample mounting inside the mono-mode circular cavity.

than the electric field in regions of predominant magnetic field [11–14]. Nowadays, the main mechanisms for microwave *H*-field heating are eddy current losses, hysteresis losses, magnetic resonance losses and residual losses [9]. Other authors englobed the magnetic resonance losses inside the residual losses, leaving three principal: eddy current losses, hysteresis losses and residual losses [15]. The eddy currents are generated in conductor materials that are exposed to a changing magnetic field during microwave processing. These eddy currents are induced in the form of close loops on all magnetic domains that are present at the surface layer of a conductor. Hysteresis loss is caused by the irreversible magnetization process in the alternating magnetic field [16]. When a magnetic material is exposed to an alternating magnetic field an oscillation of the magnetic dipoles occurs as the magnetic poles change their polar orientation. This rapid flipping generates a substantial friction and heating inside the material. The residual losses contribute to the heating but in a small proportion compared with the eddy current losses and hysteresis losses [16,17]. Domain wall resonance losses and electron spin losses are considered residual losses components [18].

Due to their ferromagnetic and electric conductivity properties $La_{0.8}Sr_{0.2}MnO_3$ materials can be sintered using both electric and magnetic fields. To this day, no studies have been found concerning the effect of a constant electric or magnetic field on the physical properties of LSM-based ceramics during sintering. The aim of this work is to study the sinterability of LSM and LSM-YSZ ceramic materials through two different microwave cavities, one with maximum *E*-field and another one with maximum *H*-field. The microstructural features and the mechanical properties are also studied in order to evaluate the possible differences caused by the different heating mechanisms.

2. Experimental procedure

2.1. Raw materials processing and conventional sintering

Commercial $La_{0.8}Sr_{0.2}MnO_3$ powder (INFRAMAT, Advanced Materials, USA) with an average particle size of $d_{50} = 0.25$ μm, a BET specific surface area of 2.8 m^2/g and a density of 6.31 g/cm^3 and commercial, high-purity yttria stabilized zirconia (YSZ) with 8 mol% Y_2O_3 (TZ8YS, Tosoh Corp., Japan), with an average particle size of 0.4 μm, a BET specific surface area of 4.7 m^2/g and a density of 5.90 g/cm^3 were used as raw materials.

The preparation of the mixtures was performed after optimizing the zeta potential of both LSM and YSZ suspensions and the rheological

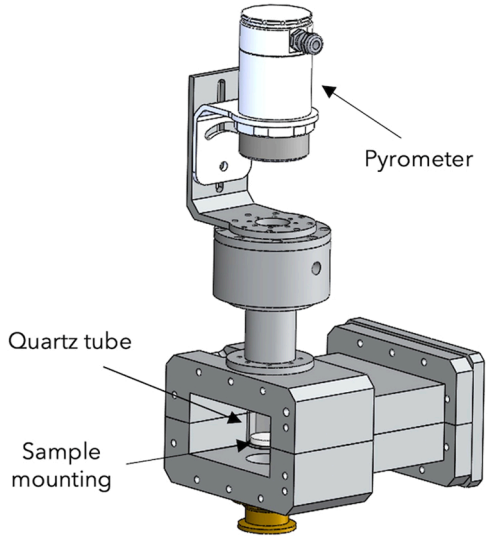

Fig. 2. Detail of the mono-mode rectangular cavity, with the pyrometer and the sample inside.

behavior of the mixture LSM-YSZ. Concentrated suspensions of LSM and LSM-YSZ were prepared in water at a solid loading of 30 vol%. The mixtures were prepared with a relative volume content of 50:50 following a sequential addition, adding first the deflocculant necessary to disperse YSZ (0.5 wt% on a dry solid basis) and then the YSZ powder, and thereafter the deflocculant needed for the LSM (1.5 wt% on a dry solid basis) prior to the LSM powder. The optimized slurry of the mixture was then frozen using a rotavapor (IKA, Germany) in a liquid-N_2 bath and subsequently freeze-dried (Cryodos-50, Telstar, Spain) at − 50 °C and 0.3 mPa for 24 h to sublimate the ice.

Freeze-dried powders were compacted by uniaxial pressing at 100 MPa in a cylindrical steel die with a height of 3 mm and a diameter of 10 mm. These compacts were sintered via conventional sintering (CS) at 1300 °C and 1400 °C with a holding time of 2 h, and a heating rate of 10 °C/min, in atmospheric conditions (air). The samples were then cooled freely to room temperature.

2.2. Design of the microwave cavities

The microwave sintering was performed using two different

experimental microwave set-ups: A single-mode cylindrical cavity operating in the TE_{111} mode with maximum *E*-field in the centre of the cavity [19] (Fig. 1), and a rectangular microwave cavity operating in the TE_{102} mode with maximum *H*-field in the centre of the cavity (Fig. 2). In both cavities, the sintering process was performed with a frequency of 2.45 GHz and using a maximum power of 350 W. The final sintering temperatures were 1200 °C and 1300 °C, with a holding time of 15 min in atmospheric conditions (air). In order to avoid thermal tensions and cracks in the samples during the sintering process it was stablished an optimum heating rate of 50 °C/min. Sintering temperatures were measured on the sample surface with the aid of an optical pyrometer (OPTRIS GmbH, Berlin, Germany) previously calibrated (emissivity) for the selected temperatures.

A key factor to obtain reproducible heating cycles with identical heating ramps is the proper insulation of the sample. Thermal insulation plays a major role since it must not only minimize the heat loss from the surface, but will help optimize power distribution between the sample and the insulating material. Xu et al. [20] reported the impact of insulation on the increase in heating rates and the reduction of temperature gradients.

As can be seen in Figs. 1 and 2, the sample is placed in the center of the cavity inside a quartz tube. Inside this tube, the sample is placed in a box surrounded by alumina fiber, which is totally transparent to microwaves and helps to create a good thermal insulation, reducing the thermal radiation on the sample. Due to the high and runaway heating microwave radiation absorption of the LSM materials, it is necessary to perform a setup for the electric and magnetic heating, as shown in Fig. 1 right (sample mounting), in which a SiC ring (very microwave absorbing material) is placed between two alumina fiber layers, to assure that the sample is not in contact with the SiC ring. Therefore, one way to avoid the heating runaway of LSM materials inside a microwave cavity is to use another material that absorbs part of the microwaves penetrating the cavity and this helps to control the LSM from absorbing all the radiation present. The susceptors are classically used to follow the heating cycle and balance the thermal field in the sample [21]. The aim is to control the heating rate of the LSM and LSM-YSZ materials homogeneously and with a controlled heating ramp of 50 °C/min.

Fig. 2 shows the magnetic heating cell, consisting of a rectangular waveguide where the resonant mode is TE_{102}. The last number (2) means that the electric field has a minimum in the center, and, consequently, there is a maximum of the magnetic field. To match the working frequency, and similarly to the circular cavity (Fig. 1), a tuning engine is located at the end of the cavity to match the resonant frequency to the one provided by the magnetron. The tuning engine consist of a movable short-circuit that tunes the cavity.

2.3. Characterization methods

The materials present electric and magnetic effects that have not been measured individually but validated by the perturbation method. It consists of introducing the sample at different positions, with a maximum of electric field, to probe the permittivity effect, and in a maximum of magnetic field, to probe the permeability effect.

The permittivity and permeability values are represented by the following complex values [22]:

$$\varepsilon' = \varepsilon_r' - j\cdot\varepsilon_r'' \qquad \mu' = \mu_r' - j\cdot\mu_r'' \tag{1}$$

Where ε_r' is the dielectric relative constant, expressing the ability of the material to store electric energy from an external source, and μ_r' the permeability relative constant measureing the ability to store magnetic energy. The imaginaries part (ε_r'' and μ_r'') are the loss factors, that indicates the ability of the material to convert this energy into heat [23].

The relative densities of specimens were determined by the Archimedes' method following the ASTM-C-373 standard [24]. Theoretical densities values of 6.57 and 6.41 g/cm^3 were used for LSM and LSM-YSZ, respectively, to estimate the relative density of the sintered specimens.

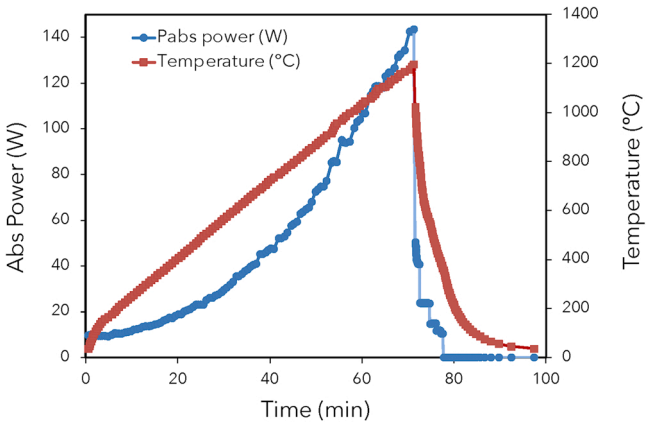

Fig. 3. Microwave absorbed power and temperature profile during heating/cooling cycle of the LSM material.

Vickers hardness, H_v, values were obtained with a Shimadzu HMV-20 micro-indenter applying a load of 2.93 N for 10 s, and 16 measurements were taken for each specimen. All samples were polished with 1 μm diamond paste for a mirror shine finish.

The microstructure and grain size were analyzed in a field emission scanning electron microscopy (FE-SEM, S4800 Hitachi, Japan). The grain size was measured using the line interception method following the ASTM E112 standard [25], with 10 interception lines being traced in each sample using Image software.

3. Results and discussion

3.1. Microwave absorbed power of the material

For the electric heating, a cavity is designed and adapted to measure the aboserbed microwave power. To carry out a study under the same conditions, the quantity of energy supplied by the equipment was monitored during the complete heating stage to avoid overheating of the material. The power supplied to the equipment was switched off during the cooling stage and the samples were cooled freely, without microwave radiation. Fig. 3 presents the absorbed microwave power profile and the temperature evolution during the complete sintering cycle (heating and cooling stage) of the LSM material. The peak power absorbed by the sample during the cycle is achieved at the maximum

Table 1
Sintering conditions, relative density and grain size of materials sintered under different heating modes.

Material	Sintering Method	Final temperature and dwell time	Relative Density (%)	Grain Size (μm)
LSM	CS	1200°C_2h	87.5 ± 0.1	1.8 ± 0.09
		1300°C_2h	94.1 ± 0.1	3.5 ± 0.07
		1400°C_2h	96.0 ± 0.1	4.3 ± 0.09
	E-MW	1200°C_15min	75.5 ± 0.1	1.7 ± 0.08
		1300°C_15min	88.2 ± 0.1	2.1 ± 0.09
	H-MW	1200°C_15min	86.3 ± 0.1	1.3 ± 0.07
		1300°C_15min	96.4 ± 0.1	2.1 ± 0.08
LSM-YSZ	CS	1200 °C_2h	88.3 ± 0.1	0.6 ± 0.03
		1300°C_2h	94.9 ± 0.1	1.5 ± 0.09
		1400°C_2h	98.1 ± 0.1	1.8 ± 0.07
	E-MW	1200°C_15min	82.3 ± 0.1	0.7 ± 0.03
		1300°C_15min	94.5 ± 0.1	1.1 ± 0.04
	H-MW	1200°C_15min	89.9 ± 0.1	0.9 ± 0.01
		1300°C_15min	97.6 ± 0.1	1.5 ± 0.07

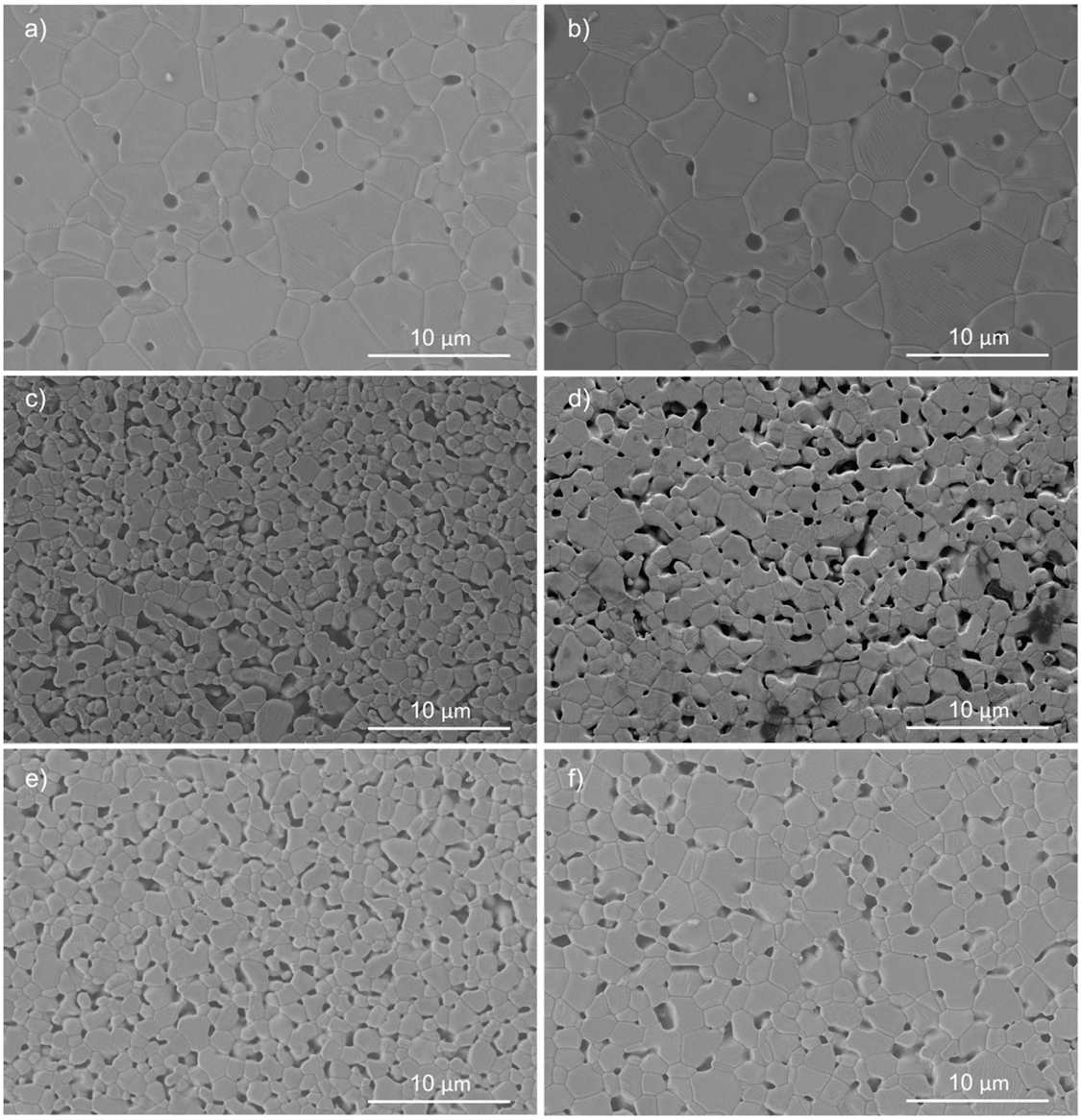

Fig. 4. FE-SEM microstructures of LSM materials sintered by conventional sintering: a) 1300ºC_2h, b) 1400 C_2h, E-MW: c) 1200°C_15min and d) 1300°C_15min and H-MW: e) 1200°C_15min and f) 1300°C_15min.

temperature (1200 ºC) and was only 140 W. The heating duration is just 70 min and all the complete cycle, until room temperature, is reduced to 90 min, at a cooling rate of 60 ºC/min. Therefore, the reduction in processing time between the conventional and microwave process is quite remarkable.

In general terms, energy absorption increases linearly with temperature until the maximum peak is reached, and no significant effect is observed. The material absorbs energy in a controlled way.

3.2. Densification and microstructural evolution

Relative density and grain size values for LSM and LSM-YSZ materials were evaluated as a function of final sintering temperature and heating mode, including; electric field (*E*-MW), magnetic field (*H*-MW) and conventional (CS). The obtained values are summarized in Table 1. It can be appreciated, for both materials, that there are significant differences in relative density and grain size behaviour depending on the heating mechanisms used. At a quick glance, it can be observed that materials obtained by microwave technology with TE_{102} mode (*H*-MW) show higher density values compared to materials obtained with TE_{111} mode (*E*-MW).

The effect of the final sintering temperature was of paramount importance, as samples sintered at lower temperature (1200 ºC) showed lower consolidation in all heating modes, either by microwave or conventional. Regarding LSM materials, the highest value of relative density (96.4%) was obtained at 1300 °C in *H*-MW, which is ~9% higher compared to that obtained in *E*-MW under the same conditions (88.2%). This value is higher than that of the same material sintered in CS at 1300 °C with a longer holding time (2 h) and very similar when using a final temperature of 1400 °C-2 h.

Figs. 4 and 5, show the FESEM microstructures of polished LSM and LSM-YSZ samples obtained by CS, *E*-MW and *H*-MW. In general, all the sintering methods follow the same trend and the largest average grain sizes were obtained at the highest sintering temperatures, where higher densification is reached. However, some residual porosity can be observed in all samples.

Grain size values of LSM materials are between 1 µm and 5 µm, approximately. It can be observed that large and small grains coexist and that at 1400 ºC by CS grain growth occurs, reaching a maximum average grain size value of 4.3 µm. At a temperature of 1300 ºC, the value

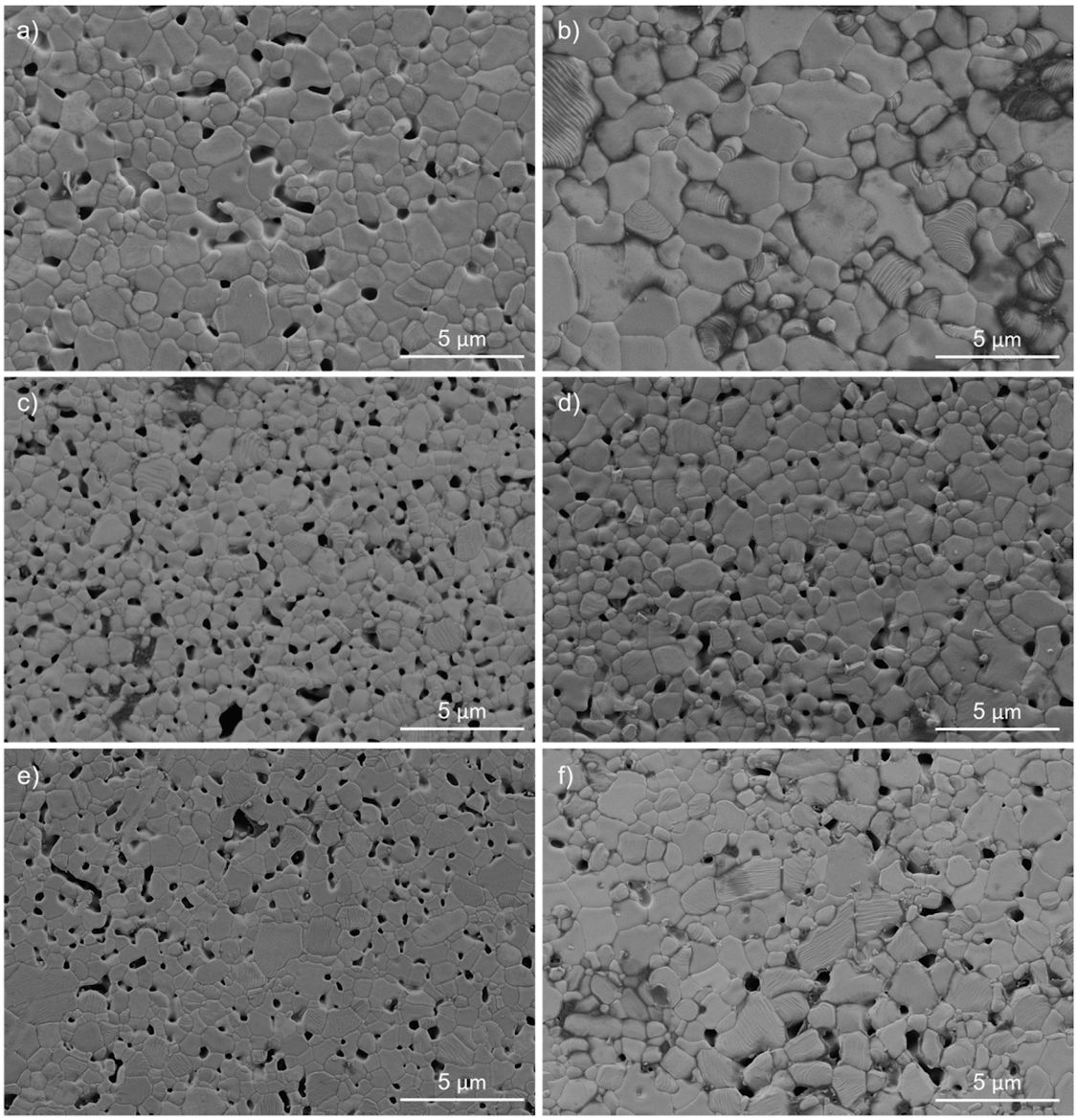

Fig. 5. FE-SEM microstructures of LSM-YSZ composites sintered by conventional sintering: a) 1300ºC_2h, b) 1400 ºC_2h, *E*-MW: c) 1200°C_15min and d) 1300°C_15min and *H*-MW: e) 1200°C_15min and f) 1300°C_15min.

obtained for the LSM sample by CS is 40% higher than that obtained by microwave in both heating modes. Therefore, the microstructure of samples obtained by microwave, using both heating modes has a much smaller grain size. Consequently, for better control of grain growth mechanisms and to obtain high densities at lower temperatures, the use of microwave sintering is very important, with emphasis on the TE_{102} heating mode.

On the contrary, as can be seen, the average grain size of the LSM-YSZ composites is much smaller than that of the LSM materials, all below 2 µm, and the introduction of a second phase of YSZ has a more significant effect on the composites obtained by CS than on those obtained by microwave. The final grain size at both 1300 °C and 1400 °C is ~60% smaller than that of the LSM materials obtained by CS (Fig. 4a and b). With respect to the composites obtained by *E*-MW and *H*-MW the grain size is 45% and 30% smaller, respectively, than LSM material (Fig. 4c, d, e and f). In general, the microstructure observed is very homogeneous and similar in all LSM-YSZ composites. The grain size obtained at 1300 ºC by CS is equivalent to that obtained by *H*-MW at 1300 ºC (1.5 µm). An important fact to consider is that LSM-YSZ composites are denser than LSM samples under all sintering conditions.

In addition, Figs. 4 and 5 show that better sintering behaviour occurs under controlled magnetic field. The densities for a 15 min holding time for the LSM-YSZ composites heated by microwave at 1300 °C in *E* and *H* field are 94.5% and 97.6%, respectively. The final densities after 120 min residence time at 1300 °C in CS are 94.9%.

Roy et al. reported that compared to conventional heating, higher mass and charge transfer occurs in *E*-MW and *H*-MW ceramics [26]. The authors reported that the different materials show different heating behaviour in the *E* and *H* field, respectively. Regarding LSM and LSM-YSZ, both can be heated using pure *E* and *H* fields, but it was observed that they show much higher absorption in the pure magnetic field, thus generating higher heating rates. In semiconductor materials, it is well accepted today that the *H*-field induces current loops that are responsible for the heating of the samples [27].

Badev et al. [15] proposed that Laplace forces act as an electromagnetic pressure induced by the combined effects of current loops under a microwave electromagnetic field. The interaction of the current loops with the *H*-field could be assumed to result in radial Laplace forces applied on the grain, which in turn leads to improved particle contact and enhances the diffusion mechanisms. This can create a

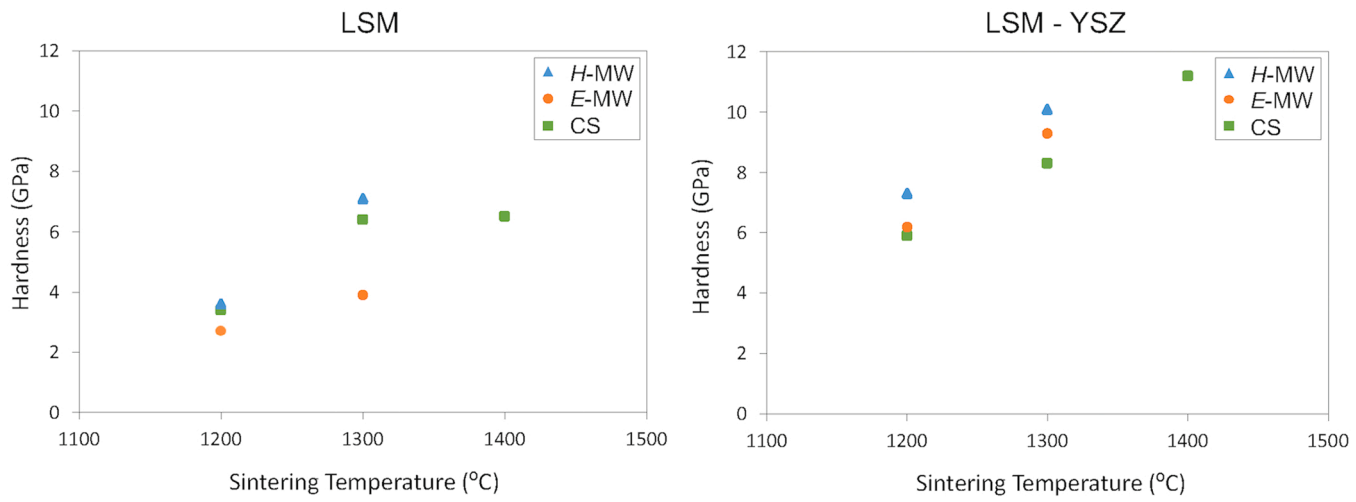

Fig. 6. Hardness vs sintering temperature of sintered LSM material and LSM-YSZ composite with different heating modes.

rearrangement of the particles in the material, thereby increasing the kinetics of densification and grain growth.

The higher relative density values obtained by the sinterability through TE_{102} microwave at the same temperature (1300 °C) enhances the importance of the magnetic losses that in the case of these materials have a huge repercussion on their densification and also on the mechanical properties that will be exposed afterwards. The basic use of these materials is as electrolyte in solid oxide fuel cells (SOFCs) components, which require about 95% of densification. Related to this, high densities have been achieved showing the high potential of the microwave sintering technique, being able to fabricate ceramics with controlled porosity by reducing the temperature and dwell times.

It is known that in conventional process the heat transfer is performed by radiation of the resistors to the sample surface and transmitted to the core through conduction. On the other hand, microwave radiation is absorbed by the material from the core of the sample to the surface; this is volumetric heating.

3.3. Hardness behaviour

Fig. 6 shows the evolution of the hardness as a function of the final sintering temperature of the LSM materials and the LSM-YSZ composites obtained by microwave technology (*E* and *H* heating-modes) in comparison with the conventional sintering method. It can be observed that the density and the final grain size obtained have an important role in achieving high hardness values. At a first glance, it can be seen that the samples with lower densities have the lowest hardness values.

In general, the LSM-YSZ composite exhibits higher hardness values compared with the LSM material. This increase in the hardness values is due to the reinforcing properties of zirconia. All composites have a hardness higher than 6 GPa, reaching maximum values $>$ 11 GPa. This is a considerable increase with respect to the LSM material, whose hardness values are in the range of $>$ 2 and ~7 GPa. On the other hand, a clear difference can be observed with respect to microwave sintered materials. LSM obtained by magnetic mode presents a hardness between 25% and 45% higher than those obtained by electrical mode at 1200 °C and 1300 °C, respectively. With respect to CS sintering, both at 1200 °C and 1300 °C, hardness values below those obtained by H-field sintering are also obtained. As discussed above, higher densities are achieved with *H*-MW cavity, thus leading to better mechanical properties. This behavior is also observed in the composite. Samples sintered by magnetic field exhibit improved hardness values, evidencing the great impact of *H*-field interaction with ferromagnetic materials such as LSM and its composites.

4. Conclusions

The sintering behaviour results of LSM and LSM-YSZ samples show that an almost fully dense ceramic with grain growth suppression can be obtained using electric and magnetic microwave sintering cycles. As compared to conventional sintering, the use of the rapid microwave heating technique led to higher densification of LSM and LSM-YSZ materials at lower sintering temperatures. The use of *H*-field microwave heating resulted in denser and more uniform microstructures in comparison to *E*-field microwave sintering. This superior heating behaviour in *H*-field is due to the field-induced current loops and the subsequent generation of Laplace forces applied to the grain, which enhances the diffusion mechanisms promoted by densification. These are very promising results facing the achievement of controlled and tailored microstructures in ceramic materials.

In summary, an efficient microwave sintering process would allow the fabrication of components with controllable macroscopic shape and structure characteristics (such as grain size). Solving such problems requires multiscale approaches and special optimization techniques. The incorporation of new advances in studies of the microwave electromagnetic field on mass transport phenomena should lead to the development and industrial mastery of a microwave sintering technology capable of producing high quality materials with novel microstructures and unique properties.

Declaration of Competing Interest

The authors declare that they have no known competing financial interests or personal relationships that could have appeared to influence the work reported in this paper.

Acknowledgements

This research was funded by the project of the Spanish Ministry of Science and Innovation: RTI2018–099033-B-C32&C33 and RYC-2016–20915, and Generalitat Valenciana (BEST/2021/084, BEST/2021/082).

References

[1] L. Zhang, Y. Zhang, Y.D. Zhen, S.P. Jiang, Lanthanum strontium manganite powders synthesized by gel-casting for solid oxide fuel cell cathode materials, J. Am. Ceram. Soc. 90 (2007) 1406–1411.
[2] N. Özbay, R.Z.Y. Şahin, Preparation and characterization of LaMnO3 and LaNiO3 perovskite type oxides by the hydrothermal synthesis method, AIP Conf. Proc. 1809 (2017).

[3] D.L. Meixner, R.A. Cutler, Sintering and mechanical characteristics of lanthanum strontium manganite, Solid State Ion. 146 (2002) 273–284.
[4] S. Harboe, Y.J. Sohn, O. Guillon, N.H. Menzler, Investigation of LSM-8YSZ cathode within an all ceramic SOFC. Part I: chemical interactions, J. Eur. Ceram. Soc. 40 (2020) 3608–3617.
[5] G. Jayakumar, D.S. Poomagal, A. Albert Irudayaraj, A. Dhayal Raj, S. Kethrin Thresa, P. Akshadha, Study on structural, magnetic and electrical properties of perovskite lanthanum strontium manganite nanoparticles, J. Mater. Sci. Mater. Electron. 31 (2020) 20945–20953.
[6] A. Princivalle, E. Djurado, Nanostructured LSM/YSZ composite cathodes for IT-SOFC: A comprehensive microstructural study by electrostatic spray deposition, Solid State Ion. 179 (2008) 1921–1928.
[7] D.K. Agrawal, Microwave processing of ceramics, Curr. Opin. Solid State Mater. Sci. 3 (1998) 480–485.
[8] R.R. Mishra, A.K. Sharma, Microwave-material interaction phenomena: Heating mechanisms, challenges and opportunities in material processing, Compos. Part A Appl. Sci. Manuf. 81 (2016) 78–97.
[9] J. Sun, W. Wang, Q. Yue, Review on microwave-matter interaction fundamentals and efficient microwave-associated heating strategies, Materials 9 (2016) 931.
[10] Z. Peng, J.Y. Hwang, M. Andriese, Magnetic loss in microwave heating, Appl. Phys. Express. 5 (2012) 8–11.
[11] Y.N. Chen, Z.J. Wang, T. Yang, Z.D. Zhang, Crystallization kinetics of amorphous lead zirconate titanate thin films in a microwave magnetic field, Acta Mater. 71 (2014) 1–10.
[12] Z. Cao, N. Yoshikawa, S. Taniguchi, Microwave heating behaviors of Si substrate materials in a single-mode cavity, Mater. Chem. Phys. 124 (2010) 900–903.
[13] R. Rosa, P. Veronesi, A. Casagrande, C. Leonelli, Microwave ignition of the combustion synthesis of aluminides and field-related effects, J. Alloys Compd. 657 (2016) 59–67.
[14] R. Roy, D. Agrawal, Radically different effects on materials by separated microwave electric and magnetic fields, Mat. Res. Innov. 5 (2002) 170–177.
[15] A. Badev, R. Heuguet, S. Marinel, Induced electromagnetic pressure during microwave sintering of ZnO in magnetic field, J. Eur. Ceram. Soc. 33 (2013) 1185–1194.
[16] Y. Zhang, Y. Zhai, Magnetic Induction Heating of Nano-sized Ferrite Particles, pp 483–500 in "Advances in Induction and Microwave Heating of Mineral and Organic Materials", S. Grundas, Ed., InTech (Croatia) 2011.
[17] R.E. Haimbaugh, "Theory of Heating by Induction", Chapter 2: Practical Induction Heat Treating, ASM International, 2001.
[18] K.I. Rybakov, E.A. Olevsky, E.V. Krikun, Microwave sintering: fundamentals and modeling, J. Am. Ceram. Soc. 96 (4) (2013) 1003–1020.
[19] R. Benavente, A. Borrell, M.D. Salvador, O. Garcia-Moreno, F.L. Peñaranda-Foix, J. M. Catala-Civera, Fabrication of near-zero thermal expansion of fully dense β eucryptite ceramics by microwave sintering, Ceram. Int. 40 (2014) 935–941.
[20] G.-F. Xu, I.K. Lloyd, Y. Carmel, T. Olorunyolemi, O.C. Wilson, Microwave sintering of ZnO at ultrahigh heating rates, J. Mater. Res. 16 (2001) 2850–2858.
[21] C. Manière, F. Borie, S. Marinel, Impact of convection and radiation on direct/hybrid heating stability of field assisted sintering, J. Manuf. Process. 56 (2020) 147–157.
[22] B. Garcia-Baños, J.M. Catalá-Civera, F.L. Peñaranda-Foix, P. Plaza-González, G. Llorens-Vallés, In situ monitoring of microwave processing of materials at high temperatures through dielectric properties measurement, Materials 9 (2016) 5.
[23] C. Delerue, M. Lannoo, Nanostructures: Theory and Modeling, Springer, New York, 2004, pp. 77–103.
[24] ASTM C373–14 Standard Test Method for Water Absorption, Bulk Density, Apparent Porosity, and Apparent Specific Gravity of Fired Whiteware Products, Astm C373–88. 88 (1999) 1–2.
[25] ASTM E112, Standard Test Methods for Determining Average Grain Size E112–10, Astm E112–10. 96 (2010) 1–27.
[26] R. Roy, R. Peelamedu, L. Hurtt, J.P. Cheng, D. Agrawal, Definitve experimental evidence for microwave effects: radically new effects of separated E and H fields, such as decrystallization of oxides in seconds, Mater. Res. Innov. 6 (3) (2002) 128–140.
[27] K. Hossbach, Investigation of the Microwave Effect, Thesis Loughborough University, November 2014.